



ELSEVIER

Earth and Planetary Science Letters 178 (2000) 59–72

EPSL

www.elsevier.com/locate/epsl

Integrated two-dimensional lithospheric conductivity modelling in the pyrenees using field-scale and laboratory measurements

Paul W.J. Glover^a, Jaume Pous^{b,*}, Pilar Queralt^b, Josep-Anton Muñoz^b,
Montserrat Liesa^c, Malcolm J. Hole^a

^a Department of Geology and Petroleum Geology, University of Aberdeen, Aberdeen AB24 3UE, UK

^b Departament de Geodinàmica i Geofísica, Universitat de Barcelona, Martí Franquès s/n, 08028 Barcelona, Spain

^c Departament de Petrologia, Geoquímica i Prospecció Geològica, Universitat de Barcelona, Martí Franquès s/n, 08028 Barcelona, Spain

Received 19 July 1999; received in revised form 3 February 2000; accepted 19 February 2000

Abstract

Recent magnetotelluric (MT) studies have shown that the lower crust in the Pyrenees contains a high conductivity zone consistent with a subducting continental slab, whose conductivity is 0.33 S/m. Partial melting has been interpreted to be the most plausible explanation for this high conductivity. Here we report a two-dimensional conductivity model of the lithosphere by integrating field-scale and laboratory determinations of the conductivity of continental crustal and mantle rocks. The laboratory data provide empirical formulas which allow us to determine the fluid saturated rock and melt conductivity when temperature, pressure and lithology are known. Consequently, we have also calculated the density, lithostatic pressure, and several alternative temperature profiles for use in the model from gravity, seismic and thermal field data. These can be used with a prescribed melt fraction to predict the electrical conductivity at depth, which can be compared with the MT conductivity data. Alternatively, the laboratory data can be combined with the MT conductivity data to predict the melt fraction at depth. The primary outputs of the modelling are conductivity and melt fraction prediction profiles for six mixing models; (i) Waff's model/Hashin–Shtrikman (HS) upper bound, (ii) HS lower bound, (iii) parallel layers, (iv) perpendicular layers, (v) random melt areas, and (vi) a modified Archie's law that takes account of the presence of two conducting phases. The modelling results indicate that a good match to the MT data can be obtained along the whole profile by the influence of pressure, temperature and the fluid phase with the only exception being the subducted slab, where a minimum of 4.7% melt fraction is necessary to explain the data. © 2000 Elsevier Science B.V. All rights reserved.

Keywords: Pyrenees; electrical conductivity; partial melting; two-dimensional models; magnetotelluric methods; conductivity; laboratory studies

1. Introduction

Magnetotelluric (MT) studies in the Pyrenees (Fig. 1) have recently noted the presence of a

* Corresponding author. Fax: +34-3-402-1340;
E-mail: jaume@natura.geo.ub.es

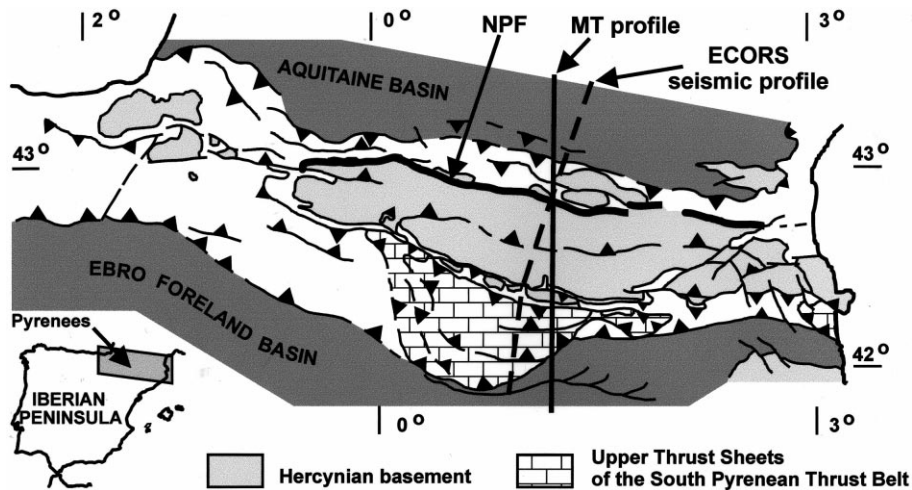


Fig. 1. Geological map of the Pyrenees showing the location of the MT line (along which the modelling has been carried out) and the ECORS seismic line [4].

high conductivity zone (0.33 S/m) that has been interpreted as partially molten subducted Iberian continental lower crust [1,2]. The subduction is a consequence of the north–south collision between the Iberian and European plates from late Cretaceous to early Miocene times. Subduction of the lower crust was inferred initially from the construction of a balanced cross-section along the ECORS–Pyrenees deep reflection seismic profile [3], which showed an upper crust 100 km longer than the lower crust. The high conductivity slab begins in the lower crust at approximately 30 km depth and at 160 km along the modelling profile (Fig. 2) and subducts towards the north retaining its high conductivity until it joins a high conductivity deep basement interpreted as aesthenosphere at 80 km depth at approximately 90 km along the modelling profile. The central Pyrenees are characterised by an asymmetric tectonic double wedge of upper crustal rocks above the subducted slab, which incorporates the North Pyrenean fault (NPF). This is a major strike-slip fault which developed during the sinistral displacement of Iberia during the Middle Cretaceous [4]. Further details of the geology can be found in [3].

Discrimination of the conduction mechanism responsible for the observed high MT conductivities in the subducted slab is currently impossible from MT data alone [1,2], or from other indirect

geophysical data [4,5]. However, the combination of MT data with lithospheric conductivity modelling from well controlled laboratory data offers a route whereby certain conduction mechanisms may be eliminated. This paper reports a new two-dimensional (2D) model of the lithosphere along the existing MT section that uses new and existing electrical conductivity data derived from laboratory measurements on a range of rock types saturated with aqueous fluids and melts subjected to lithospheric pressure and temperature conditions. This model has been used to predict the electrical conductivity at depth, and the results have been compared with conductivities observed by MT (Fig. 2a).

2. Model design

The modelling calculations have been carried out on a 2D grid 300 km long by 120 km depth, with a 10 km lateral resolution and a 5 km depth. The modelled profile (Fig. 1) is approximately coincident with the ECORS seismic profile [4], and the MT data profile [1,2], and has been tied to these laterally using the NPF as a reference (Fig. 2b). The NPF occurs at a distance of $x=100$ km in the model, where $x=0$ km is in the Aquitaine basin in France and $x=300$ km at

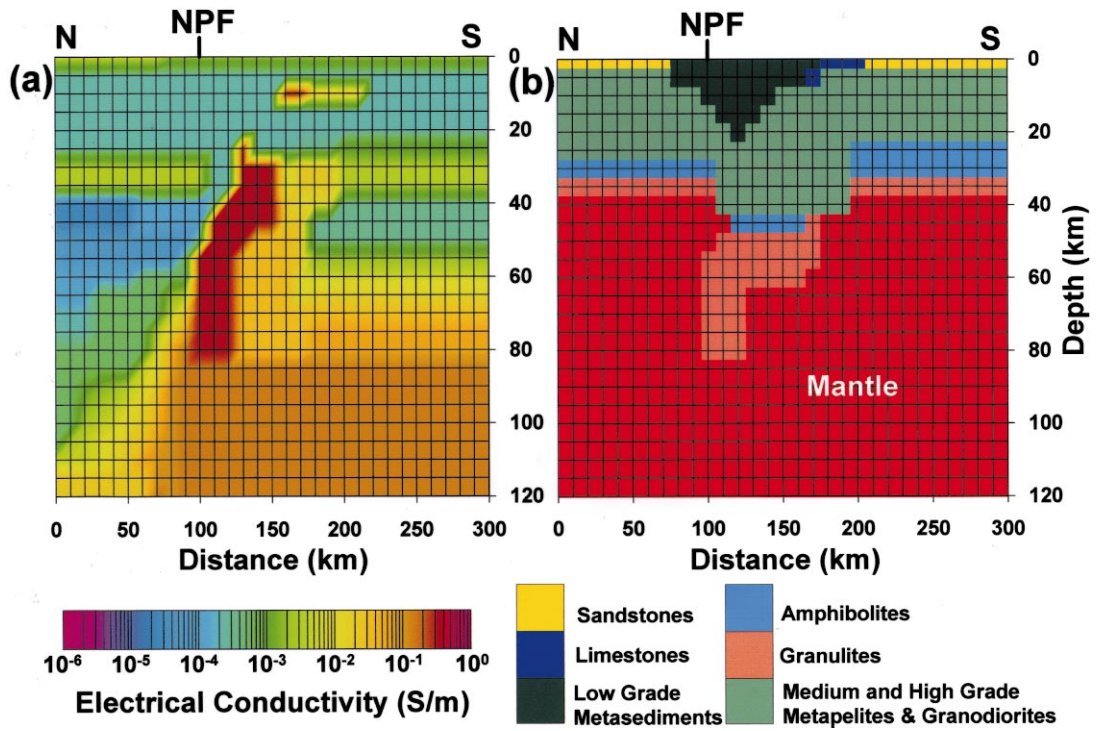


Fig. 2. (a) Conductivity profile based on MT field measurements from Pous et al. [1,2]. (b) Structure and lithology.

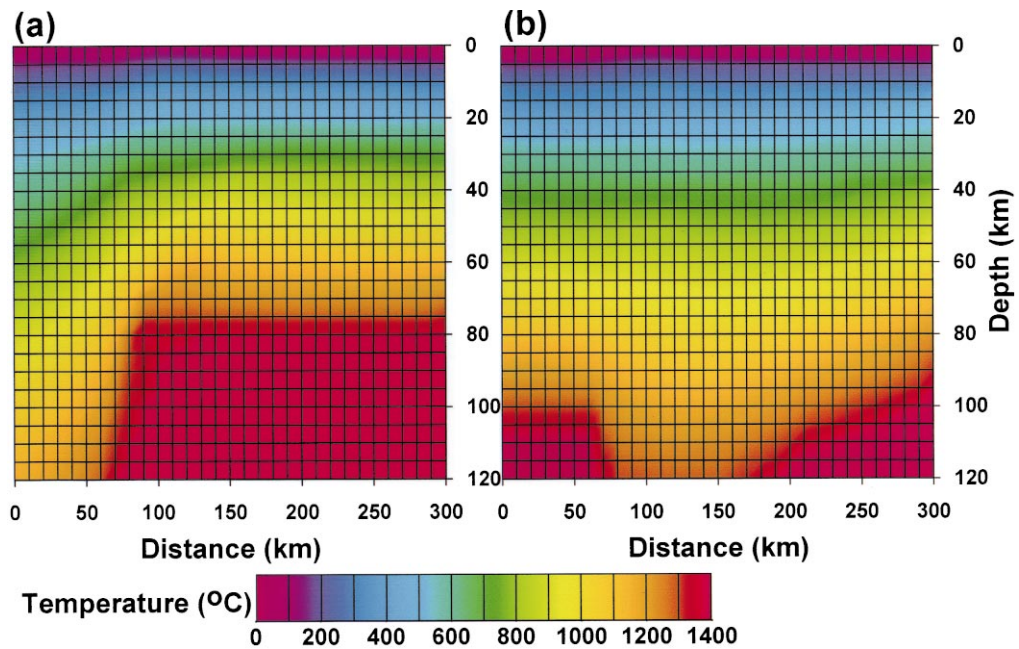


Fig. 3. (a) Calculated temperature profile, and (b) the temperature profile from the model of Zeyen and Fernandez [17].

the Catalan coastal range in Spain. Six mixing models have been used, each of which requires the input of the relevant rock matrix and melt conductivities. These are all functions of lithostatic pressure and temperature, so the temperature and pressure at each point must also be calculated.

2.1. Structure

The structure of the crust (Fig. 2b) has been taken from a seismic reflection section [4] that extends to a depth of 60 km. Interfaces between the surface sediments, upper crust, lower crust, mantle and subducting slab have been transferred from the seismic interpretation to the model grid to a depth of 60 km. Below this depth only mantle material is expected to occur, except between lateral locations 100 and 120 km at a depth of 60–80 km, where subducting slab is indicated by the MT data [1,2]. The base of the lithosphere has been delineated in accordance with the MT model. These last two constraints represent the only occurrences where the conductivity model input data are not independent of the MT data against which they will be tested.

2.2. Lithology

Lithological groups have been defined with

guidance from the materials cropping out along the modelled profile and in different cross-sections from neighbouring massifs of the Pyrenees (Fig. 2b) [6]. These are: (i) the sedimentary cover (limestones and sandstones), (ii) low metamorphic grade rocks, mainly metapelites, (iii) granodiorites and medium/high grade metapelites, (iv) amphibolites, (v) granulite facies rocks, either felsic or basic, and (vi) olivine (F_{O90}) representing mantle peridotite.

2.3. Rock matrix conductivities

Rock matrix conductivities for the surface lithologies have been measured in the laboratory with 1 M NaCl (5.84 wt%) aqueous pore fluid, and have been considered constant to a depth of 5 km for the purposes of the model. Approximately 15 fresh samples of each rock type (sandstone, limestone and metapelites) were collected along the profile. Each has been subjected to helium porosity measurement, and the mean values are given in Table 1. Each sample has been saturated with 1 M NaCl solution using vacuum and raised pressures, and has been subjected to impedance spectroscopy measurements from 50 Hz to 1 MHz at 20°C, a hydrostatic pressure of 4.08 MPa, and a pore fluid pressure of 0.68 MPa using a four electrode arrangement to remove electrode polarisation effects. All aqueous solu-

Table 1
Saturated rock matrix and melt conductivities

Rock or melt type	Source	Sample code	Porosity (%)	Fitted conductivity equation (S/m)
<i>Rock matrix</i>				
Sandstone	Laboratory measurement	Mean	8.2 ± 0.2	$\sigma_{\text{rock}} = 0.006$ (constant)
Limestone	Laboratory Measurement	Mean	5.2 ± 0.2	$\sigma_{\text{rock}} = 0.002$ (constant)
Metasediment	Laboratory Measurement	Mean	1.4 ± 0.1	$\sigma_{\text{rock}} = 0.002$ (constant) for depths ≤ 5 km $\sigma_{\text{rock}} = 0.0003$ (constant) for depths > 5 km
Granodiorite	Glover and Vine [8]	B	0.50 ± 0.1	$\sigma_{\text{rock}} = 0.128 \exp(-0.2217/k_B T) + (-0.819(P-2))$
Amphibolite	Glover and Vine [8]	E1	0.68 ± 0.1	$\sigma_{\text{rock}} = 0.164 \exp(-0.25177/k_B T) + (-0.14(P-2))$
Granulite	Glover and Vine [8]	F1	0.78 ± 0.1	$\sigma_{\text{rock}} = 0.0915 \exp(-0.25489/k_B T)$
Olivine (F _{O90})	Xu et al. [10]	H813	0.00	$\sigma_{\text{rock}} = 955 \exp(-1.73/k_B T)$
<i>Melts</i>				
Basalt mantle	Shankland and Waff [11]	–	–	$\sigma_{\text{melt}} = 18\,200 \exp(-1.147 - 4.14 \times 10^{-3} P) / k_B T$
Slab	[14,15]	–	–	$\sigma_{\text{melt}} = 30$ constant values from 0.5 to 15 S/m

Note: P = lithostatic pressure (kbar), T = temperature (K), k_B = Boltzmann's constant = 8.6171×10^{-5} eV/°C.

tions were sparged under vacuum to remove dissolved gasses prior to use. The low frequency (50 Hz) in-phase conductivity data derived from these measurements have been used for each rock type, and are given in Table 1. We have not measured or included corrections for the temperature and pressure dependence of the surface lithologies since these lithologies are represented in the model by only a surface layer a few cells thick.

Rock conductivities for the remaining major crustal lithologies (granodiorite, amphibolite, granulite) have been obtained from laboratory experiments that were carried out as a function of temperature, lithostatic pressure and pore fluid pressure, all with 100% saturation with 0.5 M NaCl (2.92 wt%) aqueous pore fluid [7,8]. The fluid with which these experiments were carried out is in the lower range of salinities for the continental crust [9] (2–10 wt%). We have corrected the reported rock conductivity values to those for rocks fully saturated with fluid salinities 1 M NaCl as a function of temperature, lithostatic pressure and pore fluid pressure assuming that the effective conductivity of the rock at a given depth, pressure and temperature is a linear function of the fluid conductivity at the same depth pressure and temperature. This salinity was chosen because it lies approximately half way between the bounds of crustal salinities given by Nesbitt [9]. Thus, we have used rock conductivities that include the effect of a 1 M NaCl fluid for the conductivity and melt predictions presented in this paper. This salinity provides a fluid conductivity of approximately 50 S/m at lower crustal depths.

The rock conductivities for the olivine ($F_{0.90}$) under upper mantle conditions have been obtained from experiments carried out as a function of temperature and pressure, and with controlled oxygen fugacity by Xu et al. [10].

The data for each major rock type have been subjected to a non-linear regression to obtain a characteristic Arrhenius equation for each rock type that depends both upon temperature and lithostatic pressure (Table 1). These equations are used in the model to calculate the rock matrix conductivity at a given grid position in the model

as a function of pressure, temperature and lithology.

2.4. Melt conductivities

The conductivity of basaltic mantle melt as a function of temperature has been taken from the work of Shankland and Waff [11], which enables a pressure and temperature dependent Arrhenius equation for the melt conductivity to be written, and hence allow the melt conductivity at a given pressure, temperature and depth in the model to be calculated, providing melt is present. The melt in the downgoing slab has been assumed to have a granitic/rhyolitic composition as it is considered to be formed as a partial melt of mainly pelitic rocks (in amphibolite or granulite facies) [6] as predicted by laboratory experiments on the melting of pelites [12,13].

For the slab we have used a range of prescribed constant melt conductivities (0.5–15 S/m) that covers the likely range of melt conductivities based on experimental data available in the literature [14,15]. The model applies the basalt melt conductivity to all grid positions in the mantle, and the granitic melt to grid positions in the crust. A cut-off temperature controls if a melt is possible for each lithology. Thus, for the crustal slab the minimum cut-off is 680°C, which is the temperature for the melting reaction involving the breakdown of muscovite at 0.5 MPa in the absence of aqueous fluids [16]. For the mantle, the cut-off temperature is 1000°C, which is less than the solidus of peridotites in order to check if melting in the mantle was required to fit the MT conductivities.

2.5. Temperature

A 2D temperature model of the lithosphere in the Pyrenees has been calculated previously by Zeyen and Fernández [17] (Fig. 3b). We have calculated a new temperature model (Fig. 3a) to be consistent with the structure derived by the MT model by using the 2D code of Zeyen and Fernández and their values of heat production and thermal conductivity. Zeyen and Fernández assumed a thickness of the lithosphere beneath Ibe-

ria of more than 100 km and an isothermic boundary condition at such a depth, our model considers the lithospheric thickness to be 80 km in Iberia, based on the MT results. However, the variation in the calculated surface heat flow between both temperature models is within the variation of the measured data [17]. The temperature models almost coincide from the surface to a depth of about 40 km, the main difference occurring at a greater depth due to the different lithospheric thickness.

2.6. Lithostatic pressure

The lithostatic pressure at depth has been calculated for each cell by using the relevant rock densities. These have been adjusted in order to fit the gravity Bouguer anomaly data and coincide with those used by Zeyen and Fernández [17], the only exception being the density of the slab beneath 50 km, where a density of 3050 kg/m³ was required to fit the Bouguer anomaly. Simple calculations using standard bulk modulus values show that the density increase due to subduction results in a slab rock density of no more than 3080 kg/m³. This is evidence that no large melt fraction is expected, otherwise a stronger negative Bouguer anomaly would be required.

3. Conductivity mixing models

A number of mixing models have been used to calculate the electrical conductivity at depth. These are (i) parallel alternating layers, (ii) perpendicular alternating layers, (iii) randomly distributed volumes of melt and rock, (iv) Waff's mixing model/Hashin–Shtrikman upper bound (HS+), (v) HS lower bound (HS-), and (vi) a modification of Archie's law that is valid for use with a conducting rock matrix such as we find deep in the crust. All six mixing models require the rock matrix conductivity, melt conductivity, and a melt fraction. The connectivity that is important for these mixing models is not necessarily the physical connectivity of the phases but the effective electrical connectivity associated with

each of the conducting phases, as the current may flow from one phase to another if the two phases have similar conductivities.

The first two models represent the physical bounds of conductivity resulting from an alternating parallel and a perpendicular arrangement of rock and melt. The randomly distributed model is a weighted geometric mean of randomly distributed volumes of rock and melt and falls between the previous two bounds. A slightly more discriminating set of bounds has been produced by Hashin and Shtrikman [18]. Waff [19] has proposed a mixing model based on a porous medium composed of composite spheres of varying size, each of which has an outer shell of melt completely covering an inner unmolten spherical core. Since the high conductivity melt of all the spheres are in contact, there is high effective connectivity of the melt phase. This model seems to make good geometrical sense if we consider partial melting in rocks to be a distributed process preferentially occurring at the grain surfaces. The Waff formula is functionally equivalent to the Hashin and Shtrikman [18] upper bound. Finally we also consider a modification to Archie's formulation valid for two conducting phases [20].

The parallel layer model describes the highest possible melt apparent connectivity and will therefore give the lowest predicted melt fraction for any given melt conductivity and observed MT-derived conductivity.

4. Modelling results

The MT conductivity model of Pous et al. [1,2] consists of rectangular blocks of constant conductivity with a marked contrast of conductivity between the blocks, while the true resistivity distribution (and the one predicted by the forward modelling) consists of a gradual variation within a lithology resulting from the continuous dependence of conductivity on temperature and pressure. This dependence can result in the presence of thin zones of high resistivity, which are not resolvable by the MT technique. This lack of resolution should be borne in mind when comparing the conductivity inferred from the MT data with

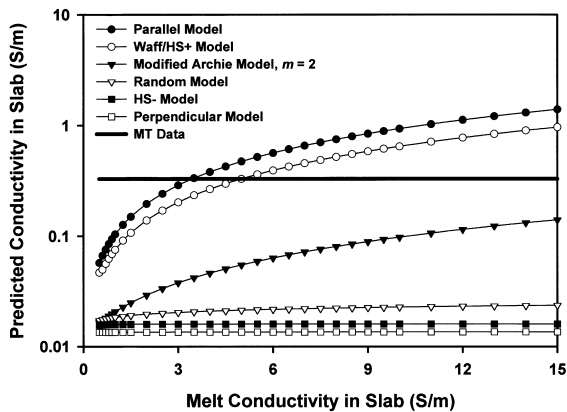


Fig. 4. Predicted conductivity in the slab as a function of melt conductivity using the six mixing models, with a melt conductivity of 5 S/m and a prescribed melt fraction of 9.4%, and compared to the observed MT conductivity in the slab.

the conductivities predicted by our forward model. Accordingly, we have used a smoothed MT model (Fig. 2a), incorporating both gradual lateral and depth resistivity variations to compare with the model's conductivity predictions and also as input to the inverse model. We have kept the MT smoothing to a minimum, and have checked that its implementation provides the same MT response as the initial MT model.

4.1. Conductivity prediction using forward modelling

The forward modelling uses laboratory data of fluid saturated rock and melt conductivities as a function of pressure and temperature for each lithology together with a prescribed melt fraction to produce a predicted conductivity profile. The predicted conductivities can then be compared with the observed MT conductivities. We have used 30 constant values for the melt conductivity of the slab (from 0.5 to 15 S/m), which are considered to include the likely range of melt conductivities at the compositions, depths, temperatures and pressures encountered in the Pyrenees. Since we are primarily interested in the conductivities in the down-going slab, we have taken the mean value of predicted conductivity over all the cells in the model representing the slab between lateral

positions 100 and 120 km and depths 55 and 80 km. These values are shown in Fig. 4 for each mixing model using a prescribed melt fraction of 9.4% and for the observed MT data. It is immediately clear that the models incorporating good melt connectivity agree reasonably well with the MT data. This is because all the curves in Fig. 4 have been calculated with a melt fraction that has been chosen to give a good fit of the Waff/HS+ conductivity prediction to the MT data for a melt conductivity of 5 S/m. The models describing partial or low connectivity do not approach the level of the MT data unless unrealistically large melt fractions are used.

Fig. 5 shows examples of the predicted conductivities along the whole profile calculated by each of the mixing models. The data can be considered in two parts; (i) the crust and mantle outside the slab, and (ii) the slab. Outside the slab, the melt fraction has been set to zero so that the predicted conductivities in the crust and mantle outside the slab depend only upon the laboratory derived measurements of fluid saturated rock conductivity. It is clear that the lithologies, fluid salinities and fluid conductivities that we have used model the conductivity of the crust and mantle outside the slab very well. This is a robust indication that our choices of laboratory derived rock conductivity data and our use of 1 M NaCl salinity fluids is valid. Within the slab a melt conductivity of 5 S/m and a melt fraction of 9.4% have been prescribed. These parameters have been chosen to ensure that the results of the HS+/Waff model (Fig. 5b) show a close correspondence to the observed MT conductivities (Fig. 2a). The parallel model slightly overestimates the observed MT conductivities as a result of the better effective connectivities implicit in the parallel model (Fig. 5a). A better correspondence between the electrical conductivities predicted by the parallel layer model and the observed MT conductivities can be achieved at slightly lower partial melt fractions (8.7%) for 5 S/m melt conductivity. The remaining models grossly underestimate the electrical conductivity in the slab (Fig. 5c–f). Unrealistic values of both partial melt fraction (approaching 100%) and melt conductivity (> 30 S/m) are required

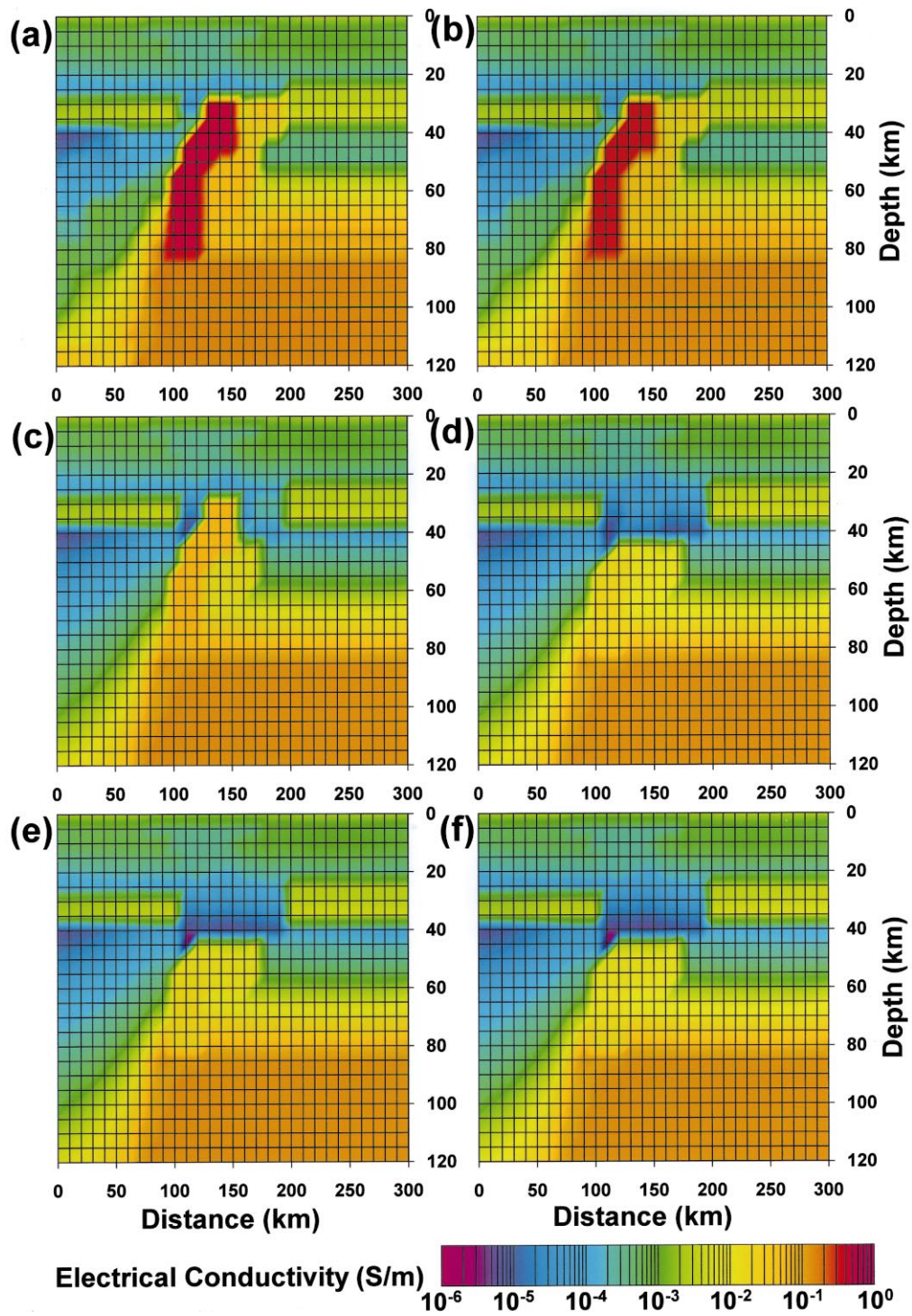


Fig. 5. Conductivity predictions for each of the six mixing models with a melt conductivity of 5 S/m and a prescribed melt fraction of 9.4%. (a) Parallel model. (b) HS+/Waff model. (c) Modified Archie's law. (d) Random melt distribution. (e) HS model. (f) Perpendicular model.

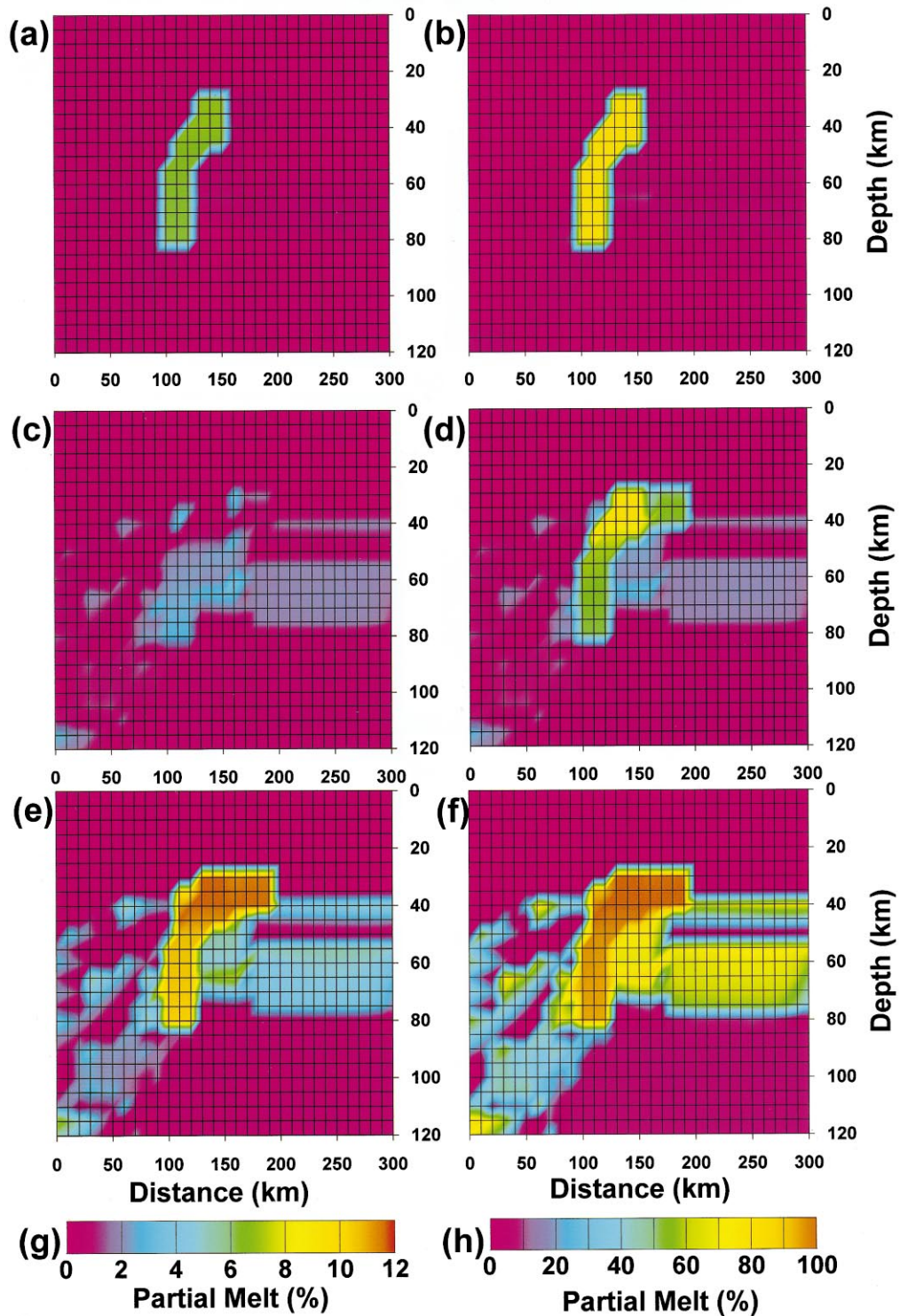


Fig. 6. Partial melt fraction (%) predictions for each of the six mixing models with a melt conductivity of 5 S/m. (a) Parallel model. (b) HS+/Waff model. (c) Modified Archie's law with $m=2$. (d) Random melt distribution. (e) HS model. (f) Perpendicular model. Colour bar (g) refers to parts (a) and (b), and colour bar (h) refers to parts (d)–(f).

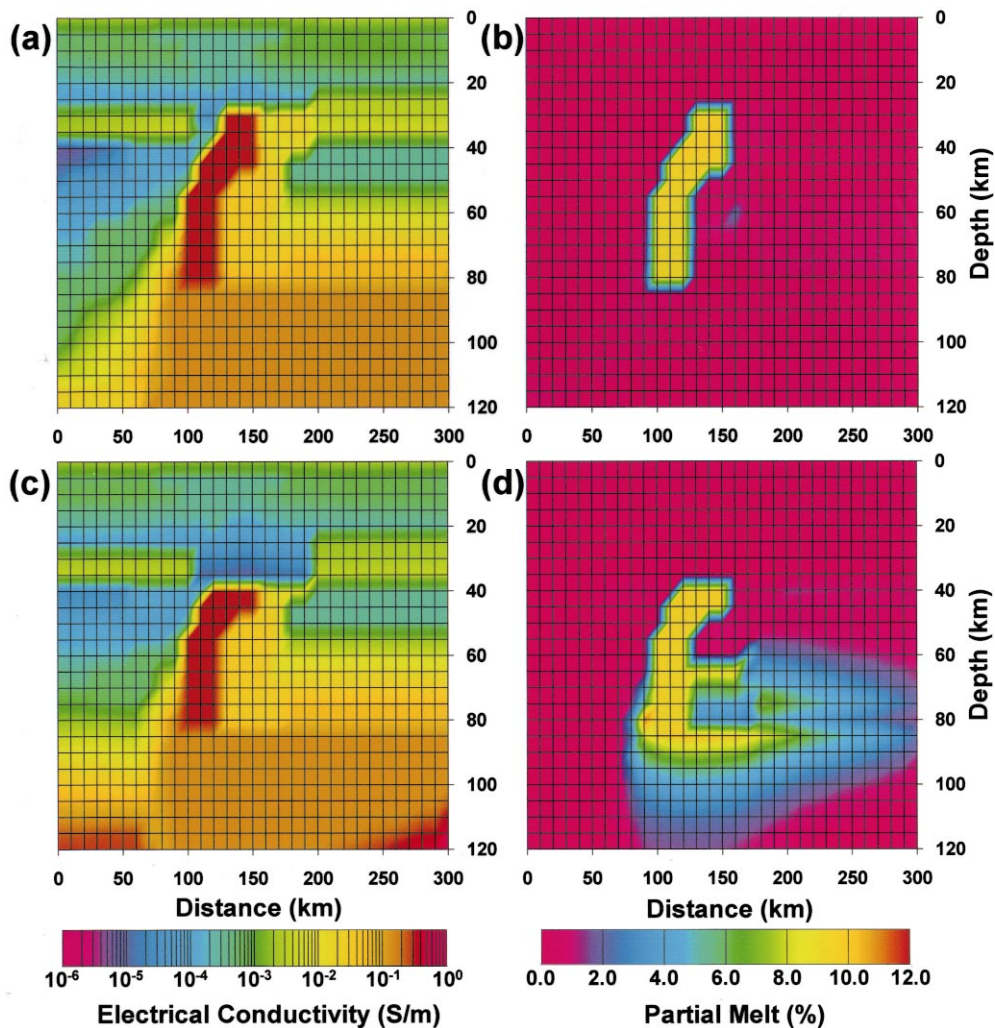


Fig. 7. Comparison of the Waff mixing model predictions of electrical conductivity and partial melt fraction for the new temperature model (a and b), and for the Zeyen and Fernández [17] temperature model (c and d). Melt conductivity = 5 S/m, melt fraction = 9.4%.

to attain the values of electrical conductivity in the slab observed by the MT measurements. Indeed, there is so little contribution to the overall conductivity by the melt for the perpendicular model (Fig. 5f), that this figure can be used to indicate the conductivities that would be present in the slab if no melt was present. Comparison of Fig. 5f with the MT conductivities (Fig. 2a) indicates clearly that for the chosen lithologies saturated with a 1 M NaCl aqueous fluid, a conduction mechanism other than fluid is required.

4.2. Melt prediction using inverse modelling

The mixing models have also been used with the conductivities of the fluid saturated rock matrix, melt conductivities and the observed MT conductivities to predict the melt fraction occurring at depth. Zones that produce zero predicted melt fraction are those where 1 M NaCl saline fluids in the rock matrix are sufficient to explain the observed conductivity at a given depth. Those zones where the predicted melt fraction is greater than zero require an additional conduction mech-

anism, which is assumed to be due to partial melting for reasons discussed later in this paper.

Fig. 6 shows the predicted partial melt fractions from such an inversion using a range of mixing models and for a slab melt conductivity set to 5 S/m. The mixing models that describe a well connected melt (the parallel layer and HS+/Waff's models) show that melt fractions in the slab are always less than 9.4% with no melt occurring elsewhere (Fig. 6a,b). The well connected melt mixing models have been tested for melt conductivities that are lower (1 and 2 S/m) and higher (7 and 10 S/m). For the 1 S/m and 2 S/m melt conductivities, the slab melt fractions are less than 41 and 22%, respectively, and for 7 S/m and 10 S/m melt conductivity the melt fractions are 6.6 and 4.7%, respectively. Mixing models describing partial effective connectivity (Fig. 6c,d) or low melt effective connectivity (Fig. 6e,f) predict unrealistically high melt fractions approaching 100% in and directly behind the slab as well as in the upper mantle. If the slab melt conductivity is set to a lower (1 or 2 S/m) or higher (7 or 10 S/m) value, the mixing models for partial and low effective connectivity melt provide predicted melt fractions that are marginally higher or lower, respectively, but still remain unrealistically high (of the order of 100%). These results are a robust indication that if melt is responsible for the high conductivities at depth, then it must exist in a substantially connected form. The lowest bound of the melt fraction occurs when well connected melt is present (parallel layer and HS+/Waff's models) with the highest melt conductivity of the melt (10 S/m).

The temperature model of Zeyen and Fernández [17] was also used in our inverse modelling. The result, shown in Fig. 7, is that even with such a colder model the melt prediction is similar in most of the slab (i.e., 9.4% for the high connectivity HS+/Waff model for a melt conductivity of 5 S/m). By contrast, the Zeyen and Fernández model also requires a small melt fraction in parts of the upper mantle in order to fit the MT conductivity, which is unrealistic bearing in mind typical values for the solidus of mantle material. A decrease of the dihedral angle of aqueous phases in the mantle would also enhance the man-

tle conductivity as proposed recently by Mibe et al. [21].

5. Discussion

The results obtained from this 2D modelling show a good agreement between the observed MT data and conductivity predictions using laboratory data saturated with saline fluids on similar lithologies to those expected in the Pyrenees at prescribed temperature and pressure conditions. The lithostatic pressure has been calculated by using densities which fit the gravity Bouguer anomaly, and the temperature has been obtained in order to fit the surface heat flow data and the geometry of the lithosphere derived by the MT data. Saline fluids are already taken into account in the rock matrix conductivity as they are considered to be the main mechanism for conductivity. However, in the deeper thickened crust (depths greater than 30 km), a conduction mechanism other than either (i) aqueous fluids at the modelled proportions, or (ii) conduction through the main mineralogies must be present to explain the high conductivities measured by MT. Higher porosities than were used in this modelling would explain the conductivity if the rocks were saturated. However, such porosities are unrealistic for lower crustal rocks [16,23] even if high pore fluid pressures are present. If the porosity remains the same as that used in the modelling, a higher conductivity fluid phase saturating the rocks would also explain the raised conductivity if the fluid is considered to be well connected. However, mineralogical considerations require that the granulites of the lower crust contain no aqueous fluid phase, suggesting that the amounts of melt required in the slab may be even higher than those indicated by the modelling. In any case, it should be noted that, for the crustal lithologies (pelitic rocks) at the PT conditions prevailing in the Pyrenean thickened crust, a partial melt would form whatever the saturation and conductivity of aqueous fluids within the original rock. This melt would quickly absorb any aqueous phase in the rock. The presence of graphite and sulphides can also be invoked to enhance conductivity. Only

small amounts are necessary, but they would have to be present in a highly connected manner over huge volumes to give the required MT conductivities [24]. In the case of graphite, it would have to be formed and remain stable over the depth and temperature range over which high melt conductivities are observed. Taking these points into consideration, it is our view that the raised conductivities studied in this modelling are most likely to derive from the presence of partial melting at depth beneath the Pyrenees.

Considering the lithological section in the Pyrenees and the temperature model, melting is possible in the deeper crust, at depths greater than 30 km. According to a number of laboratory dehydration melting experiments [12,16,22,25] the pressure and temperature conditions described in this paper at the locus of the maximum melting zone, are within the bounds of the experimental phase relations for pelite melting. In particular, the ‘melt in’ boundaries for the synthetic muscovite–biotite and muscovite–quartz experiments [25] first intersect the Pyrenean geotherm at a distance of approximately 110 km along the transect. Noting that the maximum pressure attained in the melting experiments was 15 kbar, and that the ‘melt in’ boundaries are linear, then extrapolating these boundaries to 20 or 25 kbar (~ 60 – 80 km) would result in a significant melting interval. In addition, the main phase initially controlling dehydration melting in both synthetic and natural pelites is muscovite. However, biotite will also contribute to dehydration melting after muscovite has been exhausted, such that melting can continue to considerable depths in the subducted lower crust. For locations less than ~ 100 km along the transect, melting could not occur even with extrapolation of the experimental data because the geotherm is too steep. In addition, at locations greater than ~ 160 km along the transect, crustal melting cannot occur because the depth of intersection of the geotherm with the pelite melting boundary would be in the upper mantle. Therefore on independent petrological criteria, it is clear that the most likely cause of the high conductivities is the presence of melt beneath the Pyrenees.

A lower practical bound of melt fraction (4.7%)

is inferred from our modelling and corresponds to the high connectivity (HS+/Waff mixing models) and a highest melt conductivity (10 S/m). We use the HS+/Waff model values rather than the parallel layer model values as it is considered that the Waff model represents a much more likely distribution of melt within the rock at depth. An upper bound of melt fraction is not possible to be inferred from this modelling alone given that it depends on the degree of melt effective connectivity. However, a relatively small amount of melt should be expected from the following considerations. First, the absence of collisional related volcanism in the Pyrenees may, in part, be due to a limited melt fraction being present. Melt remains in its source area until a ‘critical melt fraction’ is reached, whereupon the melt will segregate and ascend. Most authors consider the critical melt fraction to be about 20% (e.g., [16,26]). It has also been proposed that deformation enhances melt segregation by the increase of the permeability of the rock mass through vein and dyke development (e.g., [27,28]). The absence of significant post-collisional deformation in the Pyrenees indicates that surface volcanism will occur only if the melt fraction is above the critical value (20%). Secondly, the evolution and geometry of the collisional orogen and the lithological characteristics of the thickened crust also favour a limited melt fraction. Most of the magmatism at convergent orogens results from the subduction of hydrous rocks from either oceanic crust or upper continental crust. In the Pyrenees, however, oceanic crust did not exist before the collision, and crustal thickening has been accommodated by thrust-stacking of upper crustal units above a subducted lower crust [3]. Moreover, the Pyrenean orogen reworks an older crust formed during the Hercynian orogeny, which is differentiated (formed by granodiorites, amphibolite and granulite facies rocks) and has low water content at deep levels [29]. As a consequence, the combination of this distinct crustal geometry and the particular lithological characteristics may result in both the absence of free water and a limited amount of rock rich in hydrous minerals at depth. From the above considerations a melt fraction not exceeding 20% would explain the available geological

and geophysical data. In addition, if melt was present in amounts well above 10% the reduced density of the rock would produce a more negative gravity anomaly than that observed.

6. Conclusions

2D conductivity modelling has been carried out with geologically and geophysically defined inputs including laboratory data of the conductivities of fluid saturated lithologies corresponding to the Pyrenees, melt conductivity, and a range of scenarios where the melt fractions of various structural elements of the model have been varied. The modelling results indicate that a good match to the MT data can be obtained. The presence of aqueous fluids alone is sufficient to explain the majority of the upper and lower crust throughout the profile. The conductivity of the uppermost mantle can be explained fully by the conductivity of olivine (Fo₉₀) obtained from laboratory measurements, and no mantle melting is required. The subducted Iberian lower crust has an anomalously high conductivity which cannot be explained by the presence of aqueous fluids or rock matrix conduction, and is unlikely to be explained by the presence of interconnected graphite, sulphides or other conducting phases. An additional conduction mechanism is therefore required, which given the pressure and temperature conditions and crustal lithologies is interpreted as being melt. The modelling indicates that the lower bound of the melt fraction is 4.7% assuming a melt conductivity of 10 S/m and providing that the melt is well connected. The lack of surface magmatic activity in the Pyrenees is consistent with the melt fraction falling below the critical melt fraction required for melt segregation and transport to the surface, partly by the history and lithology of the Pyrenees, and partly by the lack of extensional features in the area.

Acknowledgements

We wish to thank H. Zeyen, M. Fernández, Jeff Roberts, Tom Shankland, K. Hayashi, H. Tsuka-

hara, and two anonymous referees for providing data or advice. This work was made possible by the sponsorship of Acciones Integradas (HB1997-14)/The British Council (1837) and DGICYT (PB95-269)[*FA*].

References

- [1] J. Pous, J.J. Ledo, A. Marcuello, M. Daignières, Electrical resistivity model of the crust and upper mantle from a magnetotelluric survey through the central Pyrenees, *Geophys. J. Int.* 121 (1995) 750–762.
- [2] J. Pous, J.A. Muñoz, J.J. Ledo, M. Liesa, Partial melting of subducted continental lower crust in the Pyrenees, *J. Geol. Soc.* 152 (1995) 217–220.
- [3] J.A. Muñoz, Evolution of a continental collision belt: ECORS-Pyrenees crustal balanced cross-section, in: K. McClay (Ed.), *Thrust Tectonics*, Chapman and Hall, London (1992) 235–246.
- [4] P. Choukroune, ECORS Team. The ECORS Pyrenean deep seismic profile reflection data and the overall structure of an orogenic belt, *Tectonics* 9 (1989) 23–39.
- [5] A. Souriau, A. Granet, A tomographic study of the lithosphere beneath the Pyrenees from local and teleseismic data, *J. Geophys. Res.* 100 (1995) 18117–18134.
- [6] D. Vielzeuf, Relations de phases dans le faciès granulite et implications géodynamiques, *Ann. Sci. Univ. Clermont II* 79 (1984) 1–288.
- [7] P.W.J. Glover, F.J. Vine, Electrical conductivity of carbon-bearing granulite at raised temperatures and pressures, *Nature* 360 (1992) 723–726.
- [8] P.W.J. Glover, F.J. Vine, Beyond KTB-The electrical conductivity of the deep continental crust, *Surv. Geophys.* 16 (1995) 5–36.
- [9] B.E. Nesbitt, Electrical resistivities of crustal fluids, *J. Geophys. Res.* 98 (1993) 4301–4310.
- [10] Y.S. Xu, B.T. Poe, T.J. Shankland, D.C. Rubie, Electrical conductivity of olivine, wadsleyite and ringwoodite under upper-mantle conditions, *Science* 280 (1998) 1415–1418.
- [11] T.J. Shankland, H.S. Waff, Partial melting and electrical conductivity anomalies in the upper mantle, *J. Geophys. Res.* 82 (1977) 5409–5417.
- [12] A.E. Patiño Douce, N. Harris, Experimental Constraints on Himalayan anatexis, *J. Petrol.* 39 (1998) 689–910.
- [13] J.M. Pickering, A.D. Johnston, Fluid absent melting behaviour of a two-mica metapelite: experimental constraints on the origin of the Black Hills granite, *J. Petrol.* 39 (1998) 1787–1804.
- [14] H.S. Waff, D.F. Weill, Electrical conductivity of magmatic liquids: effects of temperature, oxygen fugacity, and composition, *Earth Planet. Sci. Lett.* 28 (1975) 254–260.
- [15] J.J. Roberts, J.A. Tyburczy, Partial-melt electrical con-

- ductivity: Influence of melt composition, *J. Geophys. Res.* 104 (1999) 7055–7065.
- [16] J.D. Clemens, D. Vielzeuf, Constraints on melting and magma production in the crust, *Earth Planet. Sci. Lett.* 86 (1987) 287–306.
- [17] H. Zeyen, M. Fernández, Integrated lithospheric modelling combining thermal, gravity, and local isostasy analysis: Application to the NE Spanish Geotranssect, *J. Geophys. Res.* 99 (1994) 18089–18102.
- [18] Z. Hashin, S. Shtrikman, A variational approach to the theory of the elastic behaviour of multiphase materials, *J. Mech. Phys. Solids* 11 (1963) 12–140.
- [19] H.S. Waff, Theoretical consideration of electrical conductivity in a partially molten mantle and implications for geothermometry, *J. Geophys. Res.* 79 (1974) 4003–4010.
- [20] J.F. Hermance, The electrical conductivity of materials containing partial melts: a simple model from Archie's Law, *Geophys. Res. Lett.* 6 (1979) 613–616.
- [21] K. Mibe, T. Fujii, A. Yasuda, Control of the location of the volcanic front in island arcs by aqueous fluid connectivity in the mantle wedge, *Nature* 401 (1999) 259–262.
- [22] A.E. Patiño Douce, J.S. Beard, Dehydration-melting of biotite gneiss and quartz–amphibolite from 3 to 15 kbar, *J. Petrol.* 36 (1995) 707–738.
- [23] J.D. Clemens, G.T.R. Droop, Fluids, P–T paths and the fates of anatectic melts in the Earth's crust, *Lithos* 44 (1998) 21–36.
- [24] P.W.J. Glover, Graphite and electrical conductivity in the lower continental crust: a review, *Phys. Chem. Earth* 21 (1996) 279–287.
- [25] A.E. Patiño Douce, E.D. Humphreys, D. Johnston, Anatexis and metamorphism in tectonically thickened continental crust exemplified by the Sevier hinterland, Western North America, *Earth Planet. Sci. Lett.* 97 (1990) 290–315.
- [26] A.B. Thompson, J.A.D. Connolly, Melting of the continental crust: Some thermal and petrological constraints on anatexis in continental collision zones and other tectonic settings, *J. Geophys. Res.* 100 (1995) 15565–15579.
- [27] J.D. Clemens, C.K. Mawer, Granitic magma transport by fracture propagation, *Tectonophysics* 204 (1992) 339–360.
- [28] E.H. Rutter, The influence of deformation on the extraction of crustal melts: a consideration of the role of melt-assisted granular-flow, in: M.B. Holness (Ed.), *Deformation-enhanced Fluid Transport in the Earth's Crust and Mantle* (1997) 82–110.
- [29] D. Vielzeuf, J.D. Clemens, C. Pin, E. Moinet, Granites, Granulites and Crustal Differentiation, in: D. Vielzeuf and Ph. Vidal (Eds.), *Granulites and Crustal Evolution*, Kluwer Academic Publishers, Dordrecht (1990) 59–85.